

Fundamentals of the Plasma Sail Concept: Magnetohydrodynamic and Kinetic Studies

G. Khazanov*

NASA Marshall Space Flight Center, Huntsville, Alabama 35805

P. Delamere†

University of Colorado, Boulder, Colorado 80309

K. Kabin‡

University of Alberta, Edmonton, Alberta T6G 2J1, Canada

and

T. J. Linde§

University of Chicago, Chicago, Illinois 60637

The Mini-Magnetospheric Plasma Propulsion system (M2P2) was proposed by Winglee et al. to harness the kinetic energy of the solar wind by creating a large magnetic bubble around the spacecraft. This bubble would be supported by plasma injection into a strong magnetic field produced by an electromagnet onboard the spacecraft. In the case of M2P2, the size of the magnetic bubble is actually less than, or comparable to, the scale of these characteristic parameters. Therefore, a kinetic approach, which addresses the small-scale physical mechanisms, must be used. A two-component approach is adopted to determining a preliminary estimate of the momentum transfer to the plasma sail. The first component is a self-consistent MHD simulation of the plasma flow near the spacecraft. It is shown that the fluid treatment is valid to roughly 5 km from the source. The MHD solution is used at this boundary as initial conditions for the hybrid simulation. The hybrid simulations showed that the forces delivered to the innermost regions of the plasma sail are considerably smaller (~ 10) than their MHD counterparts. Furthermore, these forces are roughly perpendicular to the solar wind flow, in contrast to the MHD forces that are essentially aligned with the solar wind direction.

Nomenclature

B	=	magnetic field
c	=	speed of light
E	=	electric field
e	=	electronic charge
J	=	plasma current density
k	=	Boltzmann's constant
L	=	length scale
m	=	mass
N	=	dimensionless ratio
n	=	density
P	=	momentum
p	=	pressure
R, r	=	radial coordinate
S	=	surface area
T	=	temperature
t	=	time
u	=	plasma bulk flow velocity
V	=	velocity
v	=	plasma velocity
ε	=	energy density
μ_0	=	magnetic permeability of free space
ρ	=	mass density

τ	=	timescale
ω	=	plasma frequency

Subscripts

A	=	Alfvén
B	=	magnetic field
c	=	cloud
f	=	fluid
n	=	normal component
p	=	particle
pi	=	ion plasma frequency
sw	=	solar wind

Introduction

THE Mini-Magnetospheric Plasma Propulsion (M2P2), originally proposed by Winglee et al.¹ predicts that a 15-km stand-off distance (or 20-km cross-sectional dimension) of the magnetic bubble will provide for sufficient momentum transfer from the solar wind to accelerate a spacecraft to the unprecedented speeds of 50–80 km/s after an acceleration period of about three months. Such velocities will enable travel out of the solar system in period of about seven years, almost an order of magnitude improvement over present chemical-based propulsion systems. The plasma sail develops thrust to the spacecraft by absorbing momentum from the hypersonic solar wind. Coupling to the solar wind is accomplished through a magnetic bubble created by injecting plasma into a magnetic field generated by solenoid coils located on the spacecraft. The plasma sail is a new and very complicated propulsion mechanism, but it invokes specific and complex physical processes that must be studied carefully.

Winglee et al.¹ used a multifluid plasma model that treats solar wind and injected ions, as well as electrons, as separate species. Their estimation of the size of the magnetic bubble was based on extrapolation of the results obtained from several simulations of

Received 17 July 2003; revision received 15 July 2004; accepted for publication 21 July 2004. This material is declared a work of the U.S. Government and is not subject to copyright protection in the United States. Copies of this paper may be made for personal or internal use, on condition that the copier pay the \$10.00 per-copy fee to the Copyright Clearance Center, Inc., 222 Rosewood Drive, Danvers, MA 01923; include the code 0748-4658/05 \$10.00 in correspondence with the CCC.

*Airspace Engineer, National Space Science and Technology Center.

†Research Associate, Laboratory for Atmospheric and Space Physics.

‡Research Associate, Department of Physics.

§Research Scientist, Department of Astronomy and Astrophysics, 5640 S. Ellis Avenue, Chicago, IL.

systems much smaller than M2P2 (p. 21,074 of their study). We submit, however, and will show in this paper that, in the case of Winglee et al.,¹ a fluid model has no validity for such a small-scale size, even in the region near the plasma source. It is assumed in the magnetohydrodynamics (MHD) model, normally applied to planetary magnetospheres, that the characteristic scale size is much greater than the Larmor radius and ion skin depth of the solar wind. In the case of the M2P2, however, the size of the magnetic bubble is actually less than or, comparable to, the scale of these characteristic parameters. Therefore, a kinetic approach, which addresses the small-scale physical mechanisms must be used.

To our knowledge, there are currently only two preliminary attempts to use a kinetic approach to model an M2P2 system.^{2,3} Both of these efforts are based on a hybrid plasma model. The study by Saha et al.² focused on the formation of a magnetic bubble, studying the $1/r$ magnetic field dependence predicted by Winglee et al.¹ However, their work could not verify the predicted size of the M2P2. Karimabadi and Omid,³ assuming the $1/r$ magnetic field dependence as given, investigated momentum transfer from the solar wind to a magnetic bubble. They found that the degree of ion reflection needed for momentum transfer (20–50%) is approached only when the standoff distance is about 0.7 times the ion skin depth of the impinging solar wind (about 100 km). This is much larger than in the size of M2P2 device described by Winglee et al.¹ Karimabadi and Omid³ conclude that the results by Winglee et al.¹ should be reconsidered using the kinetic simulations. Note, however, that their conclusion is based on a two-dimensional model in which they use a prescribed magnetic field dependence of $1/r$ and they neglected plasma inside the magnetic bubble.

Preliminary experimental studies showed only some very simple qualitative features of the M2P2 magnetic field configuration created by expanding internal plasma and its interaction with streaming external plasma.⁴ We submit, however, that it is not possible to achieve an exact scaling of the total M2P2–solar wind interaction in the laboratory. Therefore, although these experiments provided a very qualitative picture of a magnetic bubble, because of the scaling limitations, they do not provide a useful description of the formation and characteristics of a plasma-inflated bubble required for a full-scale plasma sail.

The goal of this paper is, therefore, a focused and systematic investigation designed to elucidate the basic physical processes involved in plasma sail formation. Specifically, based on the main characteristics of the current state of knowledge of plasma sails, we will focus our investigation on three fundamental questions.

- 1) What approach should be used to describe a plasma sail formation?
- 2) What is the spatial dependence of the plasma sail's magnetic field?
- 3) What is the total force generated on the plasma sail by solar fluxes?

Each of these three issues is described in detail in the following sections. Each is crucial to the question of plasma sail feasibility, and each can be clearly identified for study by our combined MHD and kinetic theoretical approach.

Approach

The physical scale lengths associated with the plasma sail problem vary from centimeters to hundred kilometers. This is why the different approaches must be used to verify each physical principle that will be addressed in this paper. Each method, based on MHD transport equations or a kinetic description, has advantages and disadvantages. Therefore, they should not be regarded as mutually exclusive or competing approaches, but rather as complementary techniques that should all contribute to our understanding of plasma sail operation in space. To demonstrate this, we present a new combined MHD and kinetic studies of the plasma sail propulsion concept.

MHD Studies

The efficiency of the M2P2 plasma sails propulsion critically depends on if the magnetic field in the plasma bubble changes as $1/r$ starting from the coil on the spacecraft. This dependence of the magnetic field was suggested by Winglee et al.¹ based on a series of MHD simulations with the parameters significantly different from the proposed plasma sail configuration. In their simulations, Winglee et al.¹ gradually increased the magnetic field (and associated plasma injection) at the inner boundary of 10 m until it reached the strength of 4000 nT. Such a magnetic field strength and injection speed of 20 km/s lead to an ion Larmor radius of about 50 m and make fluid simulations inapplicable even in the region near the injection boundary. The $1/r$ dependence of the magnetic field was also used by Winglee et al.¹ to extrapolate the magnetic field from their inner simulation boundary of 10 m to the coil size of 10 cm. This procedure leads to the estimation that a 1-kG (0.1-T) magnetic field at the coil will result in an effective plasma sail. Thus, in view of the mentioned concerns, the conclusions reached by Winglee et al.¹ regarding the M2P2 system size and the required magnetic field strength on the spacecraft must be verified. Therefore, we have carried out the M2P2 calculations using more comprehensive theoretical tools.

The multiscale adaptive MHD model that we are using in our studies incorporates some of the most important recent advances in the numerical methods for MHD and is briefly described in Appendix A. This MHD model has been successfully applied to a variety of space plasma processes and structures, such as the comet–solar wind interaction, magnetospheres of planets and satellites, and heliosphere.^{5–8} For the Saturnian satellite Titan, the results obtained with our single-fluid MHD model were compared with the results of a quasi-multifluid model⁹ and only minor differences were found. Winglee et al. (p. 21,070) also state that overall configurations in single- and multifluid descriptions will be very similar. Such analyses justify our usage of a single-fluid MHD model for the plasma sail studies presented here.

To ensure the applicability of the MHD approach in the plasma source region, we ran this model with the magnetic field at the inner boundary ($R = 10$ m) fixed at 6×10^5 nT. This is the value suggested by Winglee et al.¹ as sufficient for the plasma sail to capture enough of the solar wind momentum to be a practical concept. We note that this estimation for the required magnetic field intensity was obtained by Winglee et al.¹ as an extrapolation of their simulations with much weaker fields, for example, 4000 nT at the 10-m inner boundary. In our simulation, the solar wind density, velocity, and temperature were chosen to be 6 cm^{-3} , 500 km/s, and 10 eV, respectively. The interplanetary magnetic field was set to 10 nT (purely in the Y direction). These parameters are fairly representative of the conditions at the Earth orbit and are similar to those used by Winglee et al.¹ At the 10-m boundary, we specified a plasma density of 1.7×10^{10} atomic mass unit/cm³, a spherical plasma outflow velocity of 20 km/s, and a plasma temperature of 5 eV. The magnetic field was set to a pure dipole with the equatorial strength at 10 m of 6×10^5 nT. All of these parameters were selected to correspond to the suggestions of Winglee et al.¹ for an operational plasma sail configuration.

Our full size M2P2 modeling results are shown in Figs. 1 and 2. Figure 1 shows the density structure on the global scale (Fig. 1a) and the region of the source (Fig. 1b). In Fig. 1, note a bow shock at about $r = 80$ km in the subsolar direction. Behind this discontinuity, the supersonic solar wind starts to divert around the obstacle presented by the plasma sail. At $r = 40$ km, there is a magnetopause that in this simulation is a discontinuity separating solar wind ions from the injected ions. Our simulated result indicates a much bigger size of the minimagnetosphere as compared to work by Winglee et al.¹ This difference can most likely be attributed to that we assumed a spherically symmetric plasma outflow at 10 m. In contrast, Winglee et al.¹ did not use symmetric loading. Other possible sources of the discrepancy may be associated with the uncertainty of the Winglee et al.¹ extrapolation and the slightly different MHD formalism assumed in the two models.

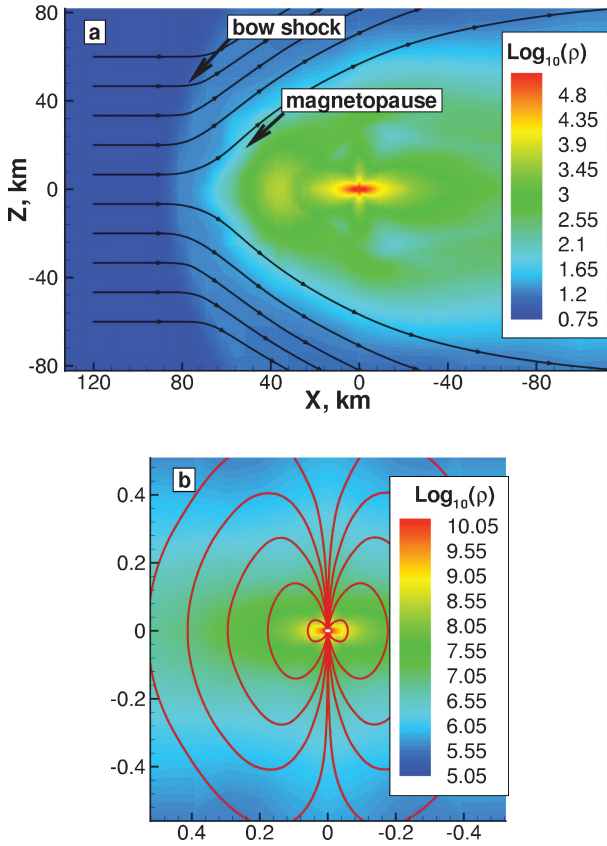


Fig. 1 Density structure from an MHD simulation a) on a global scale with solar wind flow lines that divert around magnetopause and with locations of bow shock and magnetopause and b) near region of the source with magnetic field lines.

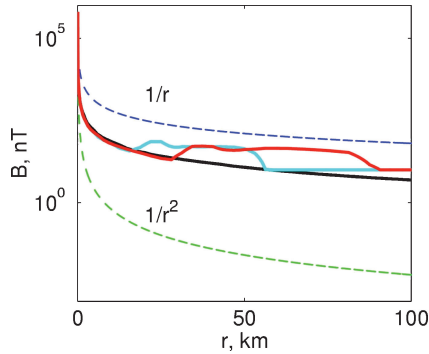


Fig. 2 Magnetic field fall off in subsolar direction: red line, MHD simulation with solar wind; black line, without solar wind; blue line, solar wind with increased dynamic pressure; and ---, $1/r$ and $1/r^2$ dependences for comparison.

Figure 2 presents the magnetic field magnitude fall off in the subsolar direction. In Fig. 2, the magnetopause appears as a sharp increase in the magnetic field intensity at 40 km as the magnetic barrier forms in the shocked solar wind plasma to counteract the expanding ejected plasma. This is the region of the most intense currents outside of the spacecraft. Magnetic forces acting between these currents and those in the coil onboard of the spacecraft are ultimately responsible for the momentum transfer between the solar wind and the plasma sail device. The bow shock in Fig. 2 is seen at about 80 km, where the magnetosheath magnetic field drops to the magnetic field value in the solar wind. The black line in Fig. 2 shows the magnetic field behavior in a simulation without the solar wind, that is, a simulation in which the injected plasma expands

into an empty space. It is seen that, up to about 25 km, the plasma expansion is unaffected by the solar wind. The distance at which the solar wind effects become noticeable obviously depends on the solar wind conditions. The blue line in Fig. 2 shows the results of a similar simulation in which the solar wind dynamic pressure was increased by a factor of three. Not surprisingly, in the simulation with the higher solar wind dynamic pressure, both the bow shock and the magnetopause are pushed closer to the spacecraft. Also, as can be seen from Fig. 2, the magnetic field has a more complicated behavior than that predicted by Winglee et al.¹ Specifically, near the region of the plasma source the magnetic field intensity falls off as $1/r^2$ and not $1/r$ as it was predicted by Winglee et al.¹ Therefore, both the magnetic field strength at the spacecraft and the electric power required to produce it are somewhat underestimated in the work of Winglee et al.¹

Our presented MHD results lead to a very important conclusion regarding the stepwise approach that can be used in our theoretical studies of plasma sail phenomena. It justifies separation of the plasma source-controlled and solar wind-controlled regions of the magnetic bubble, which can greatly simplify our theoretical studies of plasma sails. Specifically, the results from the source-controlled region can be used as the boundary conditions for kinetic simulations that must be carried out in the solar wind-controlled region of the magnetic bubble.

To ensure a smooth interface and the validity of MHD and kinetic results to be presented we have to justify the selection of the lower boundary for our kinetic studies. The first desire is to take this boundary at the distance of 25 km (where we still have source-controlled region) to avoid a large variations in scales of plasma sails and greatly simplify the numerical implementation of the kinetic code. It was not the case in our study. We selected the following criteria to be satisfied to pick this distance as far as possible from the spacecraft: 1) The characteristic-scale size at this boundary is much bigger than the Larmor radius and ion skin depth of the source. 2) Our MHD solution of source-controlled region must be valid. The first criterion is very obvious and easy to check based on the parameter values predicted by MHD solution presented in the preceding section. The second criterion required some additional scale analysis to check an applicability of the hydromagnetic approximation that is used in our MHD studies vs generalized Ohm's law. Such analysis can be performed based on the approach developed by Siscoe.¹⁰ The idea of such analysis is to compare the $\mathbf{v} \times \mathbf{B}$ term in generalized Ohm's law with all other terms and make it comfortably larger than all of them. Such comparison leads to the following dimensionless ratios of $\mathbf{v} \times \mathbf{B}$ to 1) ohmic resistance, 2) electron pressure, 3) the Hall term, and 4) electron inertia (which we have only slightly modified to reflect the nature of the plasma sail problem):

$$\begin{aligned} N_1 &= (\mu_0 e^2 / m_e) n V L_B \tau, & N_2 &= (e/k) (V B L_n / T_e) \\ N_3 &= e \mu_0 (n V L_B / B), & N_4 &= (\mu_0 e^2 / m_e) n L_B^2 \end{aligned} \quad (1)$$

In these expressions, L_B and L_n are the characteristic length of the magnetic field and plasma density, are defined as

$$L_B = \left| \frac{B}{\partial B / \partial r} \right|, \quad L_n = \left| \frac{n}{\partial n / \partial r} \right| \quad (2)$$

and are calculated based on MHD solutions. Here τ is the time between the electron and ion collisions. Figure 3 shows the calculation of N_{1-4} dimensionless ratios between 1 and 25 km. Combining these calculations with the calculations of the Larmor radius and ion skin depth of the source particles, we can comfortably place our low boundary for the kinetic simulations at the distance 5 km from the spacecraft.

Note that uniform injection of the plasma in the radial direction in a dipolar magnetic field creates toroidal electric field, which causes a continuous addition of the magnetic flux to the plasma bubble. The steady state is achieved when the rate at which the magnetic

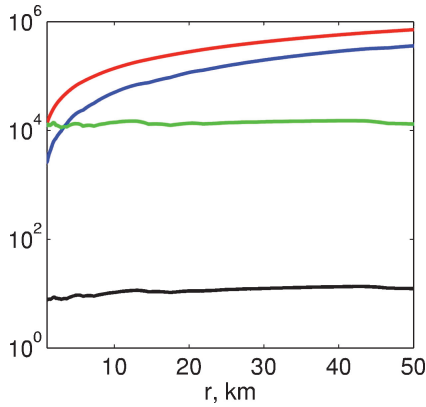


Fig. 3 Dimensionless ratios between 1 and 50 km based on an MHD simulation: red line, N_1 ; blue line, N_2 ; black line, N_3 ; and green line, N_4 .

flux is added to the system equals the rate at which it is removed by reconnection at the magnetopause. To investigate the importance of this additional magnetic flux on the system, we performed a separate MHD simulation in which plasma was injected parallel to the magnetic field lines at the inner boundary. In this case $\mathbf{v} \times \mathbf{B} = 0$, and no magnetic flux is added to the plasma bubble. The plasma injection speed was chosen to be proportional to $\cos^2(\theta)$, where θ is the magnetic latitude. Thus, the injection speed varied from 20 km/s at the magnetic pole (where the field lines are radial) to 0 at the magnetic equator, where the field lines are perpendicular to the radial direction. The results of this simulation are qualitatively very similar to our earlier results. The size of the plasma bubble is somewhat smaller than before, with the bow shock located at 50 km instead of 80 km. However, in this case the rate of plasma loss is also smaller than in the case of spherically symmetric injection. We would like to emphasize that the MHD approximation is not valid over the length scales of the plasma sail, and so all of the results of this section are only preliminary estimations to be modified and refined by kinetic simulations.

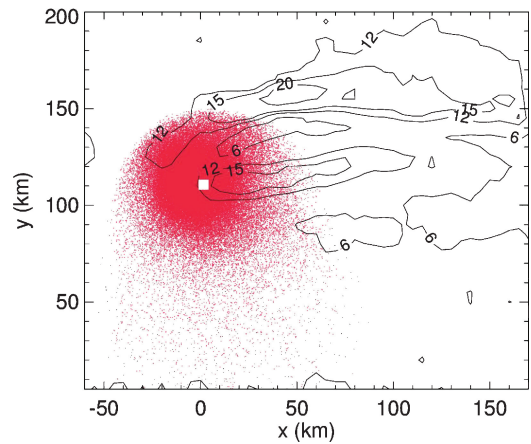
Kinetic Studies

The ion Larmor radius (hundreds of kilometers) and ion inertial length (~ 70 km) of the solar wind protons are greater than or comparable to the size of the magnetic bubble predicted by MHD studies. Therefore, it is questionable whether any of the fluid approaches should be used in describing of the momentum transfer from the solar wind to the system. Ion kinetic effects are important in a number of naturally occurring plasma systems in space plasmas. Obvious examples include the solar wind interaction with small solar system objects such as comets, planetary satellites, and small planets, for example, Mars and Pluto. Other situations in which ion kinetic effects are important include boundary regions in space. The M2P2 plasma sail system represents a similar class of problem. A critical issue facing the plasma sail concept is the role of ion kinetic effects in coupling solar wind energy and momentum to the spacecraft. Whereas the dense inner regions of the magnetic bubble may be well suited to a fluid description where the ions are strongly magnetized, the outer region of the bubble is dominated by ion kinetic effects.

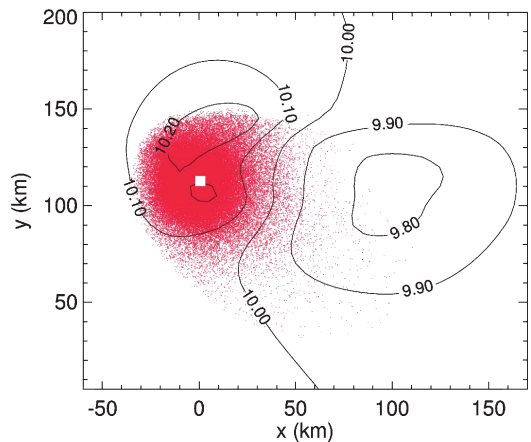
Perhaps the closest relatives to a plasma sail are the many active plasma experiments that have been conducted in Earth's space environment over the past three decades. For example, a fully three-dimensional version of the hybrid code that is used here in our plasma sail studies was originally developed by Delamere et al.^{11,12} for the plasma injection experiments made as a part of the Combined Release and Radiation Effects Satellite mission. The mathematical formalism and numerical details of this model are described in Refs. 11 and 12 and briefly outlined in Appendix B. This code is used here in our combined MHD and kinetic model.

The hybrid code provides a kinetic description for the ions and a fluid description for the electrons. A kinetic description is not necessary for the dense inner regions of the magnetic bubble, and tremendous computational savings can be realized by treating this dense, magnetized ion population with the fluid description. The hybrid simulation used the steady-state output from the MHD model interpolated to a 5-km resolution grid to specify the initial magnetic field configuration over a $5 \times 5 \times 5$ subarray centered on the source grid. The total magnetic field was then described by contributions from the fixed solar wind and MHD input magnetic fields and the perturbation magnetic fields calculated self-consistently by the hybrid code. Particles were injected from the center of the source grid into the magnetic bubble with an average injection velocity of 20 km/s such that the density in the source grid cell was maintained at the steady-state MHD value for the 5-km surface. The solar wind particles were initialized with a directed velocity of 500 km/s and randomized thermal component of 1 eV. A minimum of 10 solar wind particles per cell was maintained in the simulation. The upstream inflow boundary preserved the upstream solar wind density, whereas the downstream outflow boundary allowed particles to exit the simulation domain. All other boundaries were periodic. The simulation was run for one solar wind transit time across the simulation domain ($105 \times 45 \times 37$ grid cells). This time is sufficient to approach steady state for the innermost region of the simulation, which is the most important part of the simulation.

Figure 4 shows the position of all source particles (in red) projected onto the XY plane. Figure 4a is the case of kinetic treatment



a) Kinetic solar wind



b) Fluid solar wind

Fig. 4 Comparison of kinetic and fluid treatment of solar wind in plasma sail interaction: red contours show density of solar wind particles and source particles.

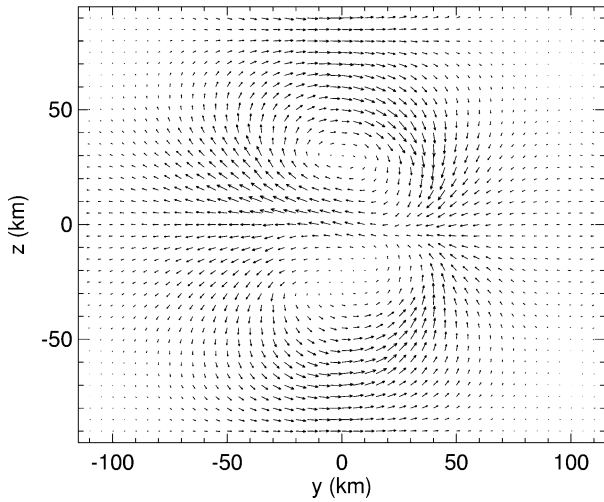


Fig. 5 Currents from hybrid simulation in downstream region perpendicular to solar wind flow direction.

of the solar wind and source particles, and Fig. 4b is the case of cold fluid treatment of the solar wind and kinetic treatment of the source population. The solar wind ion density contours are calculated for an initial density of 10 cm^{-3} .

Significant density structures developed in the wake region for the kinetic case. Two density enhancements are seen downstream as prongs. The plasma losses from the magnetic bubble also show significant differences. In Fig. 4a, the particles form two density enhancement and are lost transverse to the solar wind flow, whereas in Fig. 4b the particles are lost primarily in the downstream direction. In the case of a purely kinetic treatment of all ion particles (Fig. 4a), no upstream bow shock formed and no heating of the solar wind protons occurred throughout the interaction region. In the pure MHD case shown in Fig. 1, the plasma sail is highly symmetric. The implications of these differences between fluid and kinetic treatments are discussed in the context of momentum transfer in the next section.

Figure 5 shows the current systems from the hybrid simulation in the downstream wake region in the plane perpendicular to the solar wind flow. We note that the topology of the current system is similar to the current systems found in the Earth's magnetotail and is also similar to the current systems described by Winglee et al.¹ that couple momentum from the solar wind to the magnetic bubble. However, as we discuss in the next section, the momentum transfer in the kinetic treatment is very different from that of both the MHD and two-fluid treatments.

Momentum Transfer

Our kinetic model of the interaction between the solar wind and plasma sail illustrates the fundamental importance of ion kinetic effects in transferring momentum from the solar wind to the plasma sail. The plasma sail represents a physical system where the length scales are considerably smaller than the upstream ion inertial length. A similar interaction occurs in the case of small, magnetized asteroids. Wang and Kivelson¹³ demonstrated that the asteroid-solar wind interaction is mediated by whistler waves rather than MHD modes, that is, compressional modes and shear Alfvén waves, when the length scale of the interaction volume is smaller than the upstream ion inertial length (c/ω_{pi}). A comparison of model results with magnetometer data from the Galileo spacecraft confirmed the whistler-mediated interaction. More recently, two-dimensional hybrid code simulations by Karimabadi and Omidi³ showed that the transition from a whistler-mediated to an MHD-mediation interaction occurs for $L \approx 0.7(c/\omega_{pi})$; however, this transition may take place at even larger length scales in the three-dimensional case. The nature of momentum transfer is fundamentally different for

these two cases, as we will discuss in the context of the plasma sail application.

In the MHD approximation, the solar wind interaction with the plasma sail produces several current systems, most important of which are the magnetopause and bow shock currents. As described by, for example, Winglee et al.,¹ these currents exert magnetic forces on the spacecraft electromagnet, thus providing a momentum transfer from the solar wind to the spacecraft. A direct calculation of these forces is, however, an extremely tedious numerical procedure requiring multiple integrations over the whole three-dimensional computational volume. Fortunately, this entire procedure can be bypassed and the momentum transfer from the solar wind flow to the plasma sail can be calculated using the momentum theorem of fluid mechanics, which gives the following expression for aerodynamic force¹⁴:

$$\mathbf{F} = \iint_S \rho \mathbf{v}_n \mathbf{v} \, dS \quad (3)$$

Here S is a sufficiently large control volume enclosing the central body, \mathbf{v} is the gas or plasma velocity, and \mathbf{v}_n is the component of the velocity normal to the control volume surface.

This expression holds in MHD as well, as long as displacement currents and, therefore, momentum of the electromagnetic field is neglected. Evaluating this integral numerically, we find from our MHD simulation a force in the direction of the solar wind flow of about 5 N. Although the B_y component of the interplanetary magnetic field leads to some asymmetry of the plasma flow around the plasma sail, this asymmetry does not produce any noticeable component of the force perpendicular to the undisturbed solar wind flow.

For an MHD-mediated interaction, the momentum transfer can be understood with the frozen-in condition for magnetofluids, and the momentum transfer rate for a plasma cloud moving relative to a magnetized plasma is $dP_c/dt \approx -2\pi R_c^2 \rho v_A v_c$, where P_c is the momentum of the plasma cloud/obstacle, v_A is the local Alfvén velocity of the ambient plasma, v_c is the cloud velocity, ρ is the solar wind density, and R_c is radius of the cloud.¹² Using the model parameters for the solar wind conditions, that is, $v_{sw} = 500 \text{ km/s}$ and $n_{sw} = 6 \text{ cm}^{-3}$, we can estimate the momentum transfer to the plasma sail. Figure 1 shows that the radius of the plasma sail is roughly 40 km, so that $dP_c/dt \approx 4 \text{ N}$, in rough agreement with the MHD model calculation of 5 N. Winglee et al.¹ extrapolated their multifluid results and predicted a 20-km cross-sectional dimension and a total force of 1 N, also in agreement with our estimate. Thus, the momentum transfer mechanism, namely, the Alfvénic interaction, appears to be the same for the single- and multifluid approaches. Thus, the MHD calculations are valid for determining momentum transfer wherever the fluid approximation is valid.

The hybrid model, however, shows that the plasma sail application cannot be understood with the frozen-in condition. For an interaction dominated by ion kinetic effects, the force on the obstacle can be understood by rewriting the $\mathbf{J} \times \mathbf{B}$ force term as $(\nabla \times \mathbf{B}) \times \mathbf{B} = (\mathbf{B} \cdot \nabla)\mathbf{B} - \nabla B^2/2$. The source region of the plasma sail experiences a force due to the draping of the magnetic field over the obstacle, or tension force (first term), and a force due to magnetic pressure gradients (second term). The Alfvénic interaction generally dictates that the interaction volume will experience a uniform force due to the tension force of the draped magnetic field configuration. However, in the case of the plasma sail, the Alfvénic interaction is absent because these MHD modes cannot be excited. In this case, the currents generated by the interaction are due to the motion of pickup ions in the direction of the convection electric field, $-\mathbf{y}$. Figure 4 shows the kinetic vs fluid treatments of the solar wind flow. In the kinetic treatment (Fig. 4a), the source particles move only in the direction of the solar wind convection electric field because they do not experience a solar wind-directed magnetic tension force. In the fluid treatment (Fig. 4b), the source particles move primarily in the solar wind

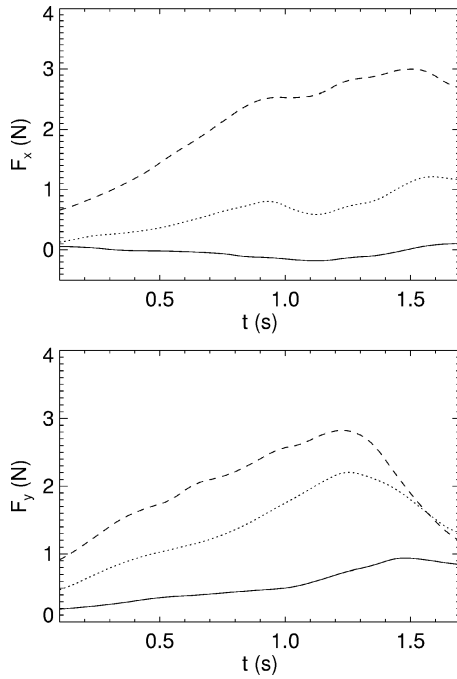


Fig. 6 Momentum transfer: total force as function of time in solar wind direction x and transverse direction y : —, $15 \times 15 \times 15 \text{ km}^3$; ---, $25 \times 25 \times 25 \text{ km}^3$; and, $35 \times 35 \times 35 \text{ km}^3$.

direction with some lateral asymmetry due to large Larmor radius effects.

The expression for momentum conservation (Appendix B) for the hybrid code states that the force on the particles in a given volume element is equal to the Maxwell stresses on the surface of the volume. (Note that the electric fields do not enter this expression due to the assumption of quasineutrality). Figure 6 shows the force on three different volume elements centered on the source region as a function of time. The solid line shows the force on a small volume containing the source grid cell ($15 \times 15 \times 15 \text{ km}^3$); the dotted and dashed lines show the force for progressively larger test volumes containing the source cell, that is, $25 \times 25 \times 25 \text{ km}^3$ and $35 \times 35 \times 35 \text{ km}^3$. Note that the force on the source grid cell is negligible, whereas the larger volumes experience larger forces due to the pickup of plasma lost from the magnetic bubble. We also note that the forces for the larger volumes asymptote to the expected analytical estimate of 1–5 N. The sudden decrease in the lateral force F_y at $t = 1.3 \text{ s}$ is due to the influence of the periodic boundary conditions and should not be considered significant. Because of the enormous computational expense of these hybrid simulations, we will investigate the steady-state nature of the plasma sail in more detail in future efforts. Figure 7 shows contours of the total magnetic field of the magnetic bubble. The source region (intersection of dotted lines) is offset from the from peak magnetic field strength. Therefore, the source region, in the absence of an accelerating tension force, will experience forces in the lateral direction $+y$ and the upstream direction $-x$ consistent with the momentum transfer calculations. For larger test volumes, the force includes the $\mathbf{J} \times \mathbf{B}$ force generated by the motion of ions picked up in the solar wind flow. A considerable lateral force is generated in the $+y$ direction consistent with the recoil of pickup ions moving in the $-y$ direction. The lateral force is analogous to the observed lateral motion of the Active Magnetospheric Particle Tracer Explorers artificial comet discussed by Delamere et al.¹¹ Thus, note the similarity between the plasma sail concept and previous active plasma experiments in space.

Future Plasma Sail Studies

An untapped resource in the plasma sail concept is the solar radiation flux (photons), which has several orders of magnitude higher force per unit area than the solar wind particle flux. For example, at 1

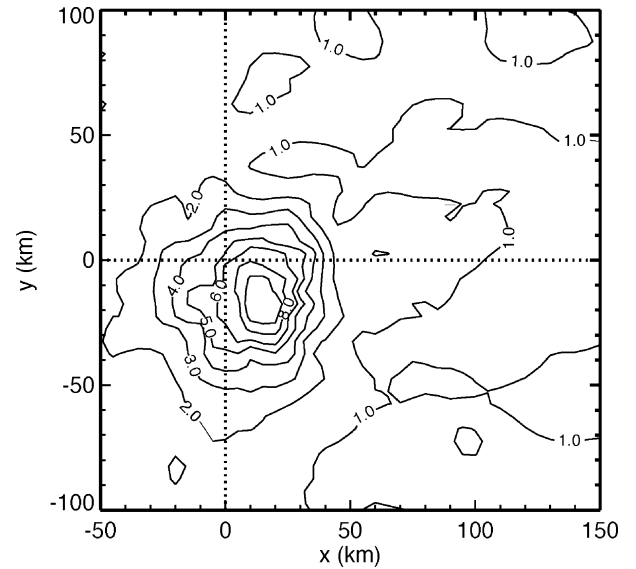


Fig. 7 Total magnetic field in the source region normalized to the interplanetary magnetic field at $t = 0.7 \text{ s}$.

astronomical unit, (AU) the solar radiation pressure is 4.57×10^{-6} vs $6.7 \times 10^{-10} \text{ (N} \cdot \text{m}^{-2})$ solar wind dynamic pressure.¹⁵ The inclusion of dust grains in a plasma bubble, which absorb or scatter solar radiation, may provide a significant improvement, or even be enabling, to plasma sail development.¹⁶ Specifically, the scattering of solar photon flux can enable 1) enhanced mission performance as a result of increased thrust, that is, increased payload and/or decreased time to destination, and 2) creation of an effective plasma sail of much smaller physical dimensions. As we have discussed, there is concern and disagreement regarding the size of a basic particle momentum transfer plasma sail required to produce a given thrust and plasma losses associated with larger systems. The latter capability will, therefore, be particularly useful if inflation and maintenance of the magnetic bubble is more difficult than predicted. Let us elaborate our considerations.

The radiation force on a $3\text{-}\mu\text{m}$ spherical SiO_2 dust grain at 1 AU is $3 \times 10^{-16} \text{ N}$ (Ref. 17), and the charge on the grain is $\sim 1500 \text{ e}$ for the expected plasma environment.¹⁶ Therefore, a force of 1 N can be achieved with 3×10^{15} dust particles. We assume that 1) the total charge on the dust is only 0.5% that of the confined plasma (to minimize influence on the plasma) and it is uniformly distributed, 2) the plasma density distribution falls off as $1/r^2$, and 3) the density of the plasma at the source is $10 \times 10^{13} \text{ cm}^{-3}$ (Ref. 1). Under these conditions, the required size of the bubble is approximately 1 km, which is an order of magnitude smaller than the most optimistic estimates of a basic plasma sail. If the P parameter, $P = 695 T_d r_d (n_d/n)$ is less than 1 (Ref. 18), the dust particles can be considered isolated, which is the case for the parameters above where the plasma temperature T_d is 0.3 eV, r_d is the grain size, and the n_d/n is the ratio of the dust to plasma densities.

The confinement of dust within a plasma bubble is the most pressing question regarding the use of dust particles. Specifically, is the dust coupled strongly enough to the field lines to confine the grains against the radiation forces and, thus, provide momentum transfer? The Larmor radius of a $3\text{-}\mu\text{m}$ dust grain with 1 m/s velocity is 30 km near the solenoid and increases rapidly with radial distance. Magnetic confinement of the dust is, therefore, not possible. If the dust is to be confined, it must be through electrostatic forces. Several such mechanisms could potentially contribute to the confinement of charged dust grains. For example, motion of a charged dust grain out of the bubble will violate quasineutrality of the confined plasma and create an electrostatic force that opposes the motion.

Discussion

The plasma sail develops thrust to the spacecraft by absorbing momentum from the hypersonic solar wind. Coupling to the solar wind is accomplished through a magnetic bubble created by injecting plasma into a magnetic field generated by solenoid coils located on the spacecraft. The plasma sail is a new and very complicated propulsion mechanism, but it invokes specific and complex physical processes.

The goal of this paper was a focused and systematic investigation that is designed to elucidate the basic physical processes involved in plasma sail formation. Specifically, based on the main characteristics of the current state of knowledge of plasma sails, we have focused our investigation on three fundamental questions.

1) What approach should be used to describe a plasma sail formation? Kinetic effects strongly dictate the nature of the momentum coupling between the solar wind and the magnetic bubble. Any approach used to describe the plasma sail formation must include these effects. However, the self-consistent description of the evolution of the plasma sail is computationally intensive and considerable savings can be realized by using a fluid treatment for the innermost regions of the magnetic bubble. The fluid description is valid inside of the 5-km boundary. That is, within the 5-km boundary the injected ions are strongly magnetized and the expansion of the magnetic bubble is largely independent of the solar wind conditions. Beyond 5 km, kinetic effects dictate the interaction, and it is critical that a kinetic approach be adopted. We have implemented a two-component approach to describe a) the self-consistent evolution of the magnetic bubble for realistic parameters and b) the momentum coupling of the bubble to the solar wind. An MHD approach was used to describe the initial expansion of the bubble, and the steady-state fluid conditions at the 5-km boundary were used as input for a hybrid code to determine the momentum coupling to the solar wind.

2) What is the spatial dependence of the plasma sail's magnetic field? Our MHD studies of the expansion of the magnetic bubble show complicated behavior ranging from $1/r^2$ to almost constant (Fig. 2). In the region near the plasma source, the magnetic field falls off initially as $1/r^2$ not $1/r$ as was predicted. The assumption of a $1/r$ magnetic field drop off near the plasma source, therefore, leads to an underestimation of the magnetic field strength needed at the spacecraft and, therefore, the required power. The expansion of the magnetic bubble is mostly unaffected by the solar wind flow out to the 25-km subsolar point.

3) What is the total force generated on the plasma sail by solar fluxes? Although our self-consistent hybrid/fluid approach to investigating the evolution and subsequent coupling of the plasma sail to the solar wind is still under investigation, our preliminary results suggest that MHD modes cannot be excited, and hence, momentum transfer to the spacecraft may be limited. However, the possibility of capturing solar radiation as a momentum source may provide a viable alternative.

Conclusions

The main motivation for and benefit of our study was to provide sufficient insight into the feasibility of the plasma sail concept. Using a two-component hybrid-MHD approach for modeling the self-consistent evolution of the magnetic bubble and the momentum coupling to the solar wind, we conclude that the momentum transfer to the spacecraft is considerably smaller than that initially predicted.¹ The pioneering study of Winglee et al.¹ assumed an MHD-mediated interaction of the plasma bubble with the solar wind. However, for MHD modes, of which Alfvén mode is most important, to be excited the cross-sectional area of the magnetic bubble has to be comparable to the upstream ion inertial length (~ 100 km). Therefore, a considerably larger plasma sail would be required for an effective tapping into the solar wind kinetic energy.

An obvious shortcoming of our model is the limited simulation domain that is computationally feasible with the three-dimensional

hybrid code. A fully kinetic approach would be desirable for describing the self-consistent evolution of the magnetic bubble, as well as improved boundary conditions for studying the steady-state configuration in the kinetic description. In addition, it will be critical to establish the scale length of the transition between a whistler-mediated and an MHD-mediated interaction in three dimensions for the plasma sail application. A discussion follows of future plasma sail studies that use solar radiation pressure as an alternative source of momentum for improving the design of the plasma sail propulsion concept.

Appendix A: MHD Equations and Numerics

The ideal MHD equations describe the conservation of mass, momentum, and energy of a conducting fluid and the evolution of the magnetic field. These equations can be written in conservative form as follows:

$$\frac{\partial \rho}{\partial t} + \nabla \cdot (\rho \mathbf{u}) = 0 \quad (\text{A1})$$

$$\frac{\partial (\rho \mathbf{u})}{\partial t} + \nabla \cdot \left[\rho \mathbf{u} \mathbf{u} + \left(p + \frac{B^2}{2\mu_0} \right) \mathbf{I} - \frac{\mathbf{B}\mathbf{B}}{\mu_0} \right] = 0 \quad (\text{A2})$$

$$\frac{\partial \mathbf{B}}{\partial t} + \nabla \cdot (\mathbf{u}\mathbf{B} - \mathbf{B}\mathbf{u}) = 0 \quad (\text{A3})$$

$$\frac{\partial \varepsilon}{\partial t} + \nabla \cdot \left[\mathbf{u} \left(\varepsilon + p + \frac{B^2}{2\mu_0} \right) - \frac{(\mathbf{u} \cdot \mathbf{B})\mathbf{B}}{\mu_0} \right] = 0 \quad (\text{A4})$$

where ρ is the plasma mass density, \mathbf{u} the plasma velocity, p the thermal pressure, and ε the total energy density given by

$$\varepsilon = \rho u^2/2 + p/(\gamma - 1) + B^2/2\mu_0 \quad (\text{A5})$$

We solve this form of the MHD equations using a modern high-resolution Godunov-type finite volume method which is described by Powell et al.¹⁹ The spatial discretization of the equations is performed on an adaptive unstructured Cartesian grid based on Octree technology.

Figure A1 shows a typical grid used in the presented MHD simulations. Note grid refinement near the bow shock in front of the plasma sail and in the inner region near the central body. Our simulations used about 500,000 cells with the sizes ranging from 50 km to 0.1 m (19 levels of refinement), which allows us to resolve well the different length scales of the problem.

The outer boundary conditions in the simulation of the solar wind interaction with the plasma sail were superfast inflow or outflow: All of the parameters are simply prescribed at the outer edge of the simulation box. In the simulation of the plasma expansion into vacuum,

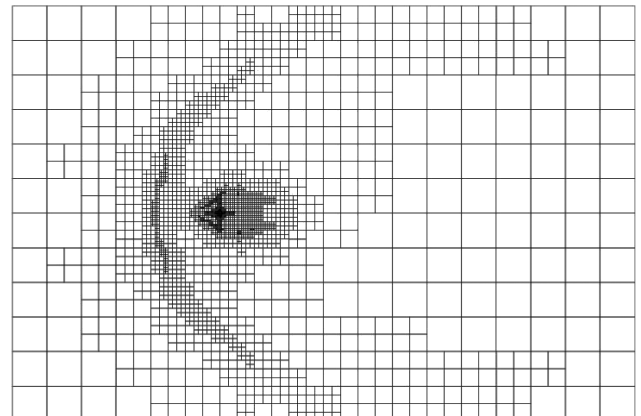


Fig. A1 Grid used for a typical MHD simulation of plasma sails.

we linearly extrapolate the MHD variables from the computational domain to the outer boundary. This allows us to mimic the infinite space beyond the simulation area and to avoid possible effects of the boundary on the computed solution. At the inner boundary we prescribed the values of the MHD variables in a layer of ghost cells just below the 10-m sphere in the same manner as described by, for example, Kabin et al.⁷

Appendix B: Hybrid Code Equations

The hybrid code was first proposed by Harned²⁰ and the particular algorithms for our code were developed by Swift.^{21,22} The code assumes quasineutrality and is nonradiative. The electric fields can be written explicitly from the electron momentum equation,

$$\mathbf{E} = -\mathbf{u}_e \times \mathbf{B} \quad (\text{B1})$$

where \mathbf{E} is the electric field in units of proton acceleration, \mathbf{B} is the magnetic field in units of ion gyrofrequency, and \mathbf{u}_e is the electron flow velocity. The electron flow speed is evaluated from Ampere's law

$$\mathbf{u}_e = \mathbf{u}_i - (\nabla \times \mathbf{B})/\alpha n \quad (\text{B2})$$

where, in mks units, $\alpha = \mu_0 e^2 / m_i$ and where m_i is the ion mass, μ_0 is the permeability of free space, and e is the electronic charge. The primary advantage for writing \mathbf{B} in units of ion gyrofrequency is that α can be used to scale the simulation particle densities to their appropriate physical values.

Faraday's law is used to update the perturbation magnetic fields,

$$\frac{\partial \mathbf{B}}{\partial t} = -\nabla \times \mathbf{E} \quad (\text{B3})$$

$$\frac{\partial \mathbf{B}}{\partial t} = -\nabla \times \left[\left(\frac{\nabla \times \mathbf{B}}{\alpha n} - \mathbf{u}_i \right) \times \mathbf{B} \right] \quad (\text{B4})$$

Note that $\mathbf{B} = \mathbf{B}_0 + \mathbf{B}_{dp} + \mathbf{B}_1$, where \mathbf{B}_0 is the ambient curl free interplanetary magnetic field, \mathbf{B}_{dp} is the curl free dipole field, and \mathbf{B}_1 is the variable field. With the equation for the magnetic fields written in this form, it can be shown that the first term on the right-hand side is responsible for the propagation of the whistler mode and the second term propagates the Alfvén modes.

The equation for the ion particle motion is

$$\frac{d\mathbf{v}}{dt} = \mathbf{E} + \mathbf{v} \times \mathbf{B} \quad (\text{B5})$$

The code also provides an optional interface between the particle ion populations and a cold fluid description where the fluid ion motion is described by

$$\frac{\partial \mathbf{u}_f}{\partial t} = \mathbf{E}_f + \frac{n_p}{n} \mathbf{u}_f \times \mathbf{B} \quad (\text{B6})$$

where

$$\mathbf{E}_f = -(\mathbf{u}_f \cdot \nabla) \mathbf{u}_f + [(\nabla \times \mathbf{B})/\alpha n - (n_p/n) \mathbf{u}_p] \times \mathbf{B} \quad (\text{B7})$$

$$\mathbf{u}_i = (n_p/n) \mathbf{u}_p + (n_f/n) \mathbf{u}_f \quad (\text{B8})$$

Momentum conservation for the hybrid code equations (no ion fluid component) is given by

$$\sum_{k=1}^{N_i} m_i \frac{d\mathbf{v}_k}{dt} = \oint_s \mathbf{T} \cdot d\mathbf{a} \quad (\text{B9})$$

where the stress tensor is

$$T_{ij} = (m_i/\alpha) \left(B_i B_j - \frac{1}{2} \delta_{ij} B^2 \right) \quad (\text{B10})$$

The total change in momentum of a given volume element is, therefore, equal to the Maxwell stress on the boundaries. The electric field does not appear in conservation expression due to the assumption of quasi neutrality.

Acknowledgment

This study was supported by the NASA In-Space Transportation Program. K. Kabin was supported by the Canadian Space Agency. We would like to thank E. Krivovitsky for many useful discussions on the topic.

References

- ¹Winglee, R. M., Slough, J., Ziemba, T., and Goodson, A., "Mini-Magnetospheric Plasma Propulsion: Tapping the Energy of the Solar Wind for Spacecraft Propulsion," *Journal of Geophysical Research*, Vol. 105, No. 9, 2000.
- ²Saha, S., Singh, N., Craven, P., Gallagher, D., and Jones, J., "Development of 3D Hybrid Code and Its Application to M2P2," *Space Technology and Applications International Forum-STAIF 2002*, edited by M. S. El-Genk, American Inst. of Physics, Albuquerque, NM, 2001, p. 441.
- ³Karimabadi, H., and Omidi, N., "Latest Advances in Hybrid Codes and Their Application to Global Magnetospheric Simulations," URL: <http://www.ssc.igpp.ucla.edu/gem/tutorial/index.html>, Geospace Environment Modeling Conf., GEM 2002.
- ⁴Winglee, R. M., Ziemba, T., Euripides, P., and Slough, J., "Magnetic Inflation Produced by the Mini-Magnetospheric Plasma Propulsion (M2P2) Prototype," *Space Technology and Applications International Forum*, Paper STAIF CP608, Feb. 2002.
- ⁵Linde, T. J., Gombosi, T. I., Roe, P. L., Powell, K. G., and DeZeeuw, D. L., "The Heliosphere in the Magnetized Local Interstellar Medium: Results of a 3D MHD Simulation," *Journal of Geophysical Research*, Vol. 103, 1998, p. 1889.
- ⁶Kabin, K., Gombosi, T. I., DeZeeuw, D. L., Powell, K. G., and Israelevich, P. L., "Interaction of the Saturnian Magnetosphere with Titan: Results of a 3D MHD Simulation," *Journal of Geophysical Research*, Vol. 104, 1999, p. 2451.
- ⁷Kabin, K., Combi, M. R., Gombosi, T. I., Nagy, A. F., DeZeeuw, D. L., and Powell, K. G., "On Europa's Magnetospheric Interaction: A MHD Simulation," *Journal of Geophysical Research*, Vol. 104, 1999, p. 19,983.
- ⁸Kabin, K., Hansen, K. C., Gombosi, T. I., Combi, M. R., Linde, T. J., DeZeeuw, D. L., Groth, C. P. T., Powell, K. G., and Nagy, A. F., "Global MHD Simulations of Space Plasma Environments: Heliosphere, Comets, Magnetospheres of Planets and Satellites," *Astrophysics and Space Science*, Vol. 274, 2000, p. 407.
- ⁹Nagy, A. F., Liu, Y., Hansen, K. C., Kabin, K., Gombosi, T. I., Combi, M. R., DeZeeuw, D. L., Powell, K. G., and Kliore, A. J., "The Interaction Between the Magnetosphere of Saturn and Titan's Ionosphere," *Journal of Geophysical Research*, Vol. 106, 2001, p. 6151.
- ¹⁰Siscoe, G. L., "Solar System Magnetohydrodynamic," *Solar-Terrestrial Physics*, Vol. 11, 1983, pp. 11–100.
- ¹¹Delamere, P. A., Swift, D. W., and Stenbaek-Nielsen, H. C., "A Three-Dimensional Hybrid Code Simulation of the December 1984 Solar Wind AMPTE Release," *Geophysical Research Letters*, Vol. 26, Sept. 1999, p. 2837.
- ¹²Delamere, P. A., Swift, D. W., Stenbaek-Nielsen, H. C., and Otto, A., "Momentum Transfer in the CRRES Plasma Injection Experiments: The Role of Parallel Electric Fields," *Physics of Plasmas*, Vol. 7, No. 9, Sept. 2000, p. 3771.
- ¹³Wang, Z., and Kivelson, M. G., "Asteroid Interaction with Solar Wind," *Journal of Geophysical Research*, Vol. 101, 1996, p. 24,479.
- ¹⁴Kueth, A. M., and Chow, C.-Y., *Foundations of Aerodynamics: Bases of Aerodynamic Design*, Wiley, New York, 1976, pp. 64–70.
- ¹⁵Parks, G., *Physics of Space Plasmas*, Addison-Wesley, Reading, MA, 1991.
- ¹⁶Sheldon, R., Thomas, E., Jr., Abbas, M., Gallagher, D., Adrian, M., and Craven, P., "Dynamic and Optical Characterization of Dusty Plasmas for Use as Solar Sails," *Space Technology and Applications International Forum-STAIF 2002*, edited by M. S. El-Genk, American Inst. of Physics, Albuquerque, NM, 2002.

¹⁷Abbas, M. M., Craven, P. D., Spann, J. F., et al., "Radiation Pressure Measurement on Micron Size Individual Dust Grains," *J. Geophys. Res.*, 2003.

¹⁸Havnes, O., Goertz, C. K., Morfill, G. E., Grun, E., and Ip, W., "Dust Charges, Cloud Potential, and Instabilities in a Dust Cloud Embedded in a Plasma," *Journal of Geophysical Research*, Vol. 92, No. A3, 1987, p. 2281.

¹⁹Powell, K. G., Roe, P. L., Linde, T. J., Gombosi, T. I., and DeZeeuw D. L., "A Solution-Adaptive Upwind Scheme for Ideal Magnetohydrodynamics," *Journal of Computational Physics*, Vol. 154, 1999,

pp. 452–462.

²⁰Harned, D. S., "Quasineutral Hybrid Simulation of Macroscopic Plasma Phenomena," *Journal of Computational Physics*, Vol. 47, 1982, p. 452.

²¹Swift, D. W., "Use of a Hybrid Code to Model the Earth's Magnetosphere," *Geophysical Research Letters*, Vol. 22, Feb. 1995, pp. 311–314.

²²Swift, D. W., "Use of a Hybrid Code for Global-Scale Plasma Simulation," *Journal of Computational Physics*, Vol. 126, 1996, pp. 109–121.